Published OnlineFirst December 5, 2013; DOI: 10.1158/0008-5472.CAN-13-2397

Cancer Research

A Preclinical Assay for Chemosensitivity in Multiple Myeloma

Zayar P. Khin[1], Maria L.C. Ribeiro[1], Timothy Jacobson[1], Lori Hazlehurst[2], Lia Perez[3], Rachid Baz[4], Kenneth Shain[4], and Ariosto S. Silva[1]

Abstract

Accurate preclinical predictions of the clinical efficacy of experimental cancer drugs are highly desired but often haphazard. Such predictions might be improved by incorporating elements of the tumor microenvironment in preclinical models by providing a more physiological setting. In generating improved xenograft models, it is generally accepted that the use of primary tumors from patients are preferable to clonal tumor cell lines. Here we describe an interdisciplinary platform to study drug response in multiple myeloma, an incurable cancer of the bone marrow. This platform uses microfluidic technology to minimize the number of cells per experiment, while incorporating three-dimensional extracellular matrix and mesenchymal cells derived from the tumor microenvironment. We used sequential imaging and a novel digital imaging analysis algorithm to quantify changes in cell viability. Computational models were used to convert experimental data into dose-exposure–response "surfaces," which offered predictive utility. Using this platform, we predicted chemosensitivity to bortezomib and melphalan, two clinical multiple myeloma treatments, in three multiple myeloma cell lines and seven patient-derived primary multiple myeloma cell populations. We also demonstrated how this system could be used to investigate environment-mediated drug resistance and drug combinations that target it. This interdisciplinary preclinical assay is capable of generating quantitative data that can be used in computational models of clinical response, demonstrating its utility as a tool to contribute to personalized oncology. *Cancer Res; 74(1); 56–67. ©2013 AACR.*

Major Findings

By designing an experimental platform with the specific intent of generating experimental parameters for a computational clinical model of personalized therapy in multiple myeloma, while taking in consideration the limitations of working with patient primary cells, and the need to incorporate elements of the tumor microenvironment, we have generated patient-individualized estimations of initial response and time to relapse to chemotherapeutic agents.

Introduction

The purposes of preclinical systems range from early identification of compounds with anticancer activity, estimation of patient-specific clinical response, or the discovery of novel targetable cellular mechanisms (6, 7). All available systems have strengths and limitations: *in vitro* assays using cell lines are scalable, reproducible, and inexpensive, but cell lines are significantly different from their originating tumors (8), and the tumor microenvironment's effects are often absent in these assays. Animal models include more realistic elements such as drug pharmacokinetics and influence of the tumor microenvironment, but they often rely on cell lines, require long-term experiments, and carry significant financial cost. Irrespective of the preclinical model used, the data generated cannot be directly ported into clinical estimations without the help of an adequate computational framework.

Computational modeling has long been used to study the dynamics of tumor response to therapy, as well as emergence of drug resistance (9–11). These theoretical models are powerful tools for analyzing complex interactions like the tumor-host-therapy system, and could, in a near future, become decision-support systems for oncologists, making personalized oncology a possibility (12). The Achilles' heel of such models, however, is the reliability of the experimental data used to parameterize them. More often than not, these computational models are parameterized by data from literature, in many cases from experiments that have been performed at incompatible conditions.

We propose that preclinical assays, specifically designed to generate data to parameterize such computational models, would significantly advance the field. Such assays, however, should comply with minimum requirements: (i) compatibility with patient primary cancer cells; (ii) recapitulate the tumor microenvironment, namely extra-cellular matrix and stroma; (iii) be nondestructive, so longitudinal studies can be performed, incorporating the temporal dimension; (iv) require as

Authors' Affiliations: Departments of [1]Cancer Imaging and Metabolism, [2]Molecular Oncology, [3]Bone Marrow Transplantation, and [4]Department of Hematologic Malignancies, H. Lee Moffitt Cancer Center and Research Institute, Tampa, Florida

Note: Supplementary data for this article are available at Cancer Research Online (http://cancerres.aacrjournals.org/).

Corresponding Author: Ariosto Silva, H. Lee Moffitt Cancer Center, 12902 Magnolia Dr, SRB4, Tampa, FL 33612. Phone: 813-745-8205; Fax: 813-745-8375; E-mail: ariosto.silva@moffitt.org

doi: 10.1158/0008-5472.CAN-13-2397

Published OnlineFirst December 5, 2013; DOI: 10.1158/0008-5472.CAN-13-2397

Quick Guide to Equations and Assumptions

Analysis of experimental data

The default function of dose–response was written as equation A, and the data points were the normalized viability in each region of interest (ROI) at a given time point and drug concentration:

$$\text{Viability}(\%) = 100 \times \frac{2^{\Delta T/T}}{\left(1 + \left(\frac{Rx}{\text{IC}_{50\,Rx}}\right)^{\exp Rx} \times \left(\frac{\Delta T}{\text{IC}_{50\,\Delta T}}\right)^{\exp T}\right)}. \quad \text{(A)}$$

The goodness-of-fit was calculated from a linear regression of the points of the fit equation with the actual observed experimental points using Prism 5 (GraphPad) and quantifying the slope and R^2 of the regression. The complete Matlab code is available in the Supplementary Material. For each example, two hypotheses were tested: either the sample was composed of 1 or 2 subpopulations. When no significant differences were observed in R^2, the simplest model was used (1 population).

Equation A is the simplest expression that describes how a homogenous population of multiple myeloma cells responds to chemotherapy as a function of concentration and exposure time. A growth term was included in the numerator of equation A, where T is the doubling time and ΔT is the variable representing drug exposure time. Rx represents the drug concentration to which cells are exposed, whereas IC_{50Rx}, $\text{IC}_{50\Delta T}$, exp Rx, and exp T are constants that determine the drug concentration and exposure time that causes death of 50% of the multiple myeloma cells and the steepness of the slope of the viability curve, respectively.

The alkylating agent melphalan has a short half-life in media and *in vivo* of approximately 2 hours, mainly because of hydrolysis (1). We have observed, however, that in long-term experiments, cells continue to die a week after melphalan exposure (see Results). For this class of drugs, we have created a mathematical expression that encompasses drug half-life, DNA damage, and DNA damage–induced cell death (equation B).

$$\begin{aligned} Viab\,(\%) &= 100 \times Death \times Growth \\ Death &= \frac{1}{1+\frac{\text{CumulDamage}^{\exp \text{IC}_{50}}}{\text{IC}_{50}}} \\ CumulDamage(t+\mathrm{d}t) &= CumulDamage(t) + \left(\int Rx\,\mathrm{d}t\right)^{\exp \text{DMG}} \cdot \\ Growth(t) &= 2^{\frac{t}{T \times [1+CumulDamage(t) \times K_T]}} \\ Rx(t) &= Rx_0 \times 2^{-\frac{t}{T_{\text{Mel}}}} \end{aligned} \quad \text{(B)}$$

"Death" and "Growth" are the two functions that determine the changes in number of viable cells in a given drug concentration, at a certain time point. "Death" represents the probability that any given cell from a population will die as a function of accumulated DNA damage ("CumulDamage"), which in turn is proportional to the area under the curve (AUC) of drug concentration Rx and exposure time dt. "exp DMG" is an empirical exponent. "Growth" quantifies cell replication, which depends on the drug-free doubling time T, the amount of DNA damage "CumulDamage," and an empirical proportional constant K_T. In other words, DNA damage slows replication (2). The last expression means that the concentration of active melphalan in media, Rx, decays with a half-life T_{Mel} of 2 hours.

Equation B is an empirical expression, with the goal of interpolating the data points across time and concentration dimensions, while recapitulating known mechanisms of melphalan toxicity and degradation. It is not, however, the only possible expression possible, and it may not properly compute the viability in concentrations or exposure times significantly higher than the experimental conditions.

Computational modeling of therapy

In this computational model, one or more subpopulations are represented, each with a size, a doubling time, and a level of sensitivity to the chemotherapeutic agent tested. Carrying capacity, which is the maximum theoretical growth rate of the entire tumor burden, was estimated from the labeling index commonly observed in multiple myeloma patients (~1–3%). Intratumoral competition was modeled by an equation that determines that bigger populations have higher chance of replicating than smaller ones (equation C), a dynamic similar to genetic drift.

$$N_i(t+\mathrm{d}t) = N_i(t) \times \left(1 + \left(\frac{Rx}{\text{IC}_{50\,Rx_i}}\right)^{\exp Rx_i} \times \left(\frac{\mathrm{d}t}{\text{IC}_{50\,\Delta T_i}}\right)^{\exp T_i}\right)^{-1} \times \left\{\left[(1+\text{LI})^{\frac{\mathrm{d}t}{T_i}} - 1\right] \frac{\times N_i(t)}{\sum N_j(t)} + 1\right\}. \quad \text{(C)}$$

Published OnlineFirst December 5, 2013; DOI: 10.1158/0008-5472.CAN-13-2397

Equation C describes how the size of a subpopulation within the tumor burden (N_i) changes within an interval of time (dt) in response of drug-induced cell death induced by exposure to a drug at the concentration Rx for the interval of time dt. The surviving cells may replicate at a rate determined by their labeling index (LI), the duration of their cell cycle (T), and the percentage that the subpopulation represents in the total tumor burden.

Bortezomib concentration in blood is characterized by a peak of ~100 nmol/L, followed by a sharp decrease, and a stable concentration of ~1 to 3 nmol/L between 2 and 192 hours after intravenous administration (1.3 mg/m^2; refs. 3, 4). The *in vitro* chemosensitivity data from patients 8, 11, 12, and 13 parameterized the computational models of clinical response for each of these patients in a hypothetical single-agent bortezomib regimen, in which the bone marrow concentration would remain constant at 3 nmol/L.

As a preliminary validation of the correlation between *in vitro* and *in vivo* chemosensitivity, we have used computational models parameterized by assays with the human multiple myeloma cell line NCI-H929 to estimate the response to bortezomib treatment of a subcutaneous mouse model treated with 1 mg/kg bortezomib bi-weekly (5). Pharmacokinetic studies have shown that such intravenous injections in mice cause a peak blood concentration of ~0.5 nmol/L and ~0.4 nmol/L at 48 hours. For these simulations, we consider a stable 0.4 nmol/L concentration of bortezomib in the bone marrow of these mice along the treatment. NCI-H929 cells have a cell cycle of approximately 24 hours, and in the subcutaneous model, the tumors have a doubling time of approximately 3.5 days, indicating that in this animal model, approximately 20% of H929 cells are actively replicating at a given time, which was used as labeling index in the simulations.

few cells per experimental condition as possible, so each patient sample could be tested against a panel of chemotherapeutic agents, in different environmental conditions; and (v) the data generated should result in testable clinical predictions, such as the depth of response and/or progression-free survival (PFS).

Four decades ago, Salmon and colleagues (13) proposed an *in vitro* method for estimation of clinical response of patients with cancer based on the capacity of primary cancer cells to form colonies at physiologically reachable chemotherapy concentrations. The main limitation of these early assays, however, was the small number of patient samples that were capable of forming colonies under control conditions. With a cloning efficiency between 0.001% and 0.1%, the growth of colonies *in vitro* was a challenge comparable to surviving the chemotherapeutic insult itself. Consequently, these restrictions limited the number of drugs, concentrations, and time points that could be studied for a single patient (14), even in more recent models (15). Finally, the outcome of these assays were often dichotomized, in other words, either a patient was "sensitive" or "resistant" to the drug, but no information was provided regarding duration of response and time to relapse. Given that in many cancers the overall survival is more dependent on the duration of the response than on its depth (16, 17), the application of these early assays as predictive biomarkers was somewhat limited.

Similar to Leonardo Da Vinci's "aerial screw," designed in the 15th century, which only came to fruition as the helicopter 5 centuries later, we propose that Salmon's drug sensitivity assay was hindered by technological limitations of its time, not by an inherent design fault. Building on this pioneering work, we here describe a novel approach for preclinical assessment of drug efficacy. We apply this method to multiple myeloma, an incurable plasma cell malignancy in which cancer cells uncontrollably proliferate in the bone marrow. Adhesion to bone marrow's extracellular matrix or stroma has been shown to confer *de novo* multidrug resistance [environment-mediated drug resistance (EMDR); refs. 18, 19].

The here described system combines a microfluidic dose–response platform, for *in vitro* screening of drugs, and a computational model of clinical response. The *in vitro* component consists of a 3-dimensional (3D) reconstruction of the bone marrow microenvironment, including primary multiple myeloma cells, extracellular matrix, and patient-derived stroma and growth factors. Live microscopy and digital image analysis are used to detect cell death events in different drug concentrations, which are used to generate dose–response surfaces. The *in silico* component is an evolutionary computational model designed to simulate how a heterogeneous population of cancer cells responds to therapy. From the *in vitro* data, the model identifies the size and chemosensitivity of subpopulations within the patient's tumor burden, and simulates how the tumor would respond to the drug(s) in physiological conditions in a clinical regimen.

The main innovations of this platform are: (i) small number of cancer cells required (1,000–10,000 per experiment); (ii) assessment of drug efficacy in different environmental conditions (collagen ± patient stroma ± patient-derived growth factors/cytokines), allowing quantification of innate and environmental drug resistance; (iii) only bright field imaging is used, thus no toxicity from viability markers; (iv) continuous imaging provides drug effect as a function of concentration and exposure time; and (v) the integration between *in vitro* and computational evolutionary models, to estimate clinical outcome: not only the initial response, but also PFS, a more relevant clinical endpoint for assessment of drug efficacy (16).

In this article, we describe the experimental and computational platforms, the results with human myeloma cells lines, and how they compare with literature data. We also describe preliminary experiments with patient primary cells, and how these results could be used in the estimation of clinical efficacy of experimental drugs, or personalized medicine (the right drugs and the right regimen for each patient).

Published OnlineFirst December 5, 2013; DOI: 10.1158/0008-5472.CAN-13-2397

Materials and Methods

Cell lines

The human myeloma cell lines RPMI-8226, HS-5/GFP-labeled, NCI-H929, and 8226/LR-5 were kindly provided by Dr. William Dalton's laboratory. The 8226/dsRed2 cell line was stably transfected with the fluorescent protein dsRed2. All cells were maintained in culture with RPMI 1640 (Gibco) media supplemented with 10% heat inactivated FBS (Life Technologies) and 1% penicillin–streptomycin solution (Invitrogen), in incubators at 5% CO_2, 37°C. Melphalan-resistant 8226/LR-5 cells were maintained in 5 μmol/L melphalan in medium, and cultured in drug-free medium for 2 weeks before the experiments.

Primary cancer cells

We investigated the *in vitro* response of cancer cells from 7 patients with multiple myeloma in the clinical trial MCC# 14745 conducted at the H. Lee Moffitt Cancer Center and Research Institute, as approved by the Institutional Review Board. The medical records were deidentified and only the following clinical-relevant information was reviewed: (i) treatment administered (chemotherapeutic agents, doses, and schedule) before biopsy; (ii) cytogenetics; and (iii) blood and urine electrophoresis results. Patients in trial MCC# 14745 received standard-of-care treatment, and consented to provide an extra sample of bone marrow aspirate during a routine biopsy. These aspirates were used in the *in vitro* assays further described. After informed written consent, bone marrow aspirates were obtained from patients with multiple myeloma either newly diagnosed or with refractory disease. Processing of bone marrow aspirate and selection of multiple myeloma cells is described in Supplementary Material. Multiple myeloma cells were seeded into the Ibidi μ-slide Chemotaxis 3D device under experimental culture conditions (described below) within 4 hours of each patient biopsy.

In vitro procedures

Drugs. In this work, the following chemotherapeutic agents were tested: bortezomib (acquired from Selleckchem), melphalan (from Sigma), and fluorescent molecule fluorescein (FAM)-HYD-1 (kindly provided by Dr. Hazlehurst).

In vitro dose–response assays in 3D microfluidic chambers. Commercially available 3D cell-culture slides (μ-slide Chemotaxis 3D *Ibitreat* from Ibidi, LLC) were gas and temperature equilibrated at 37°C, 5% CO_2 overnight before cell seeding. Each slide is composed of 3 separate chambers each with a 1-mm wide, 50-μm high cell-viewing chamber that holds a volume of 6 μL. It is connected to two 65 μL reservoirs along both sides. Linear chemical gradients form across the cell chamber via passive diffusion. Aliquots consisting of 6.67 μL 10× MEM (Life Technologies), 6.67 μL deionized H_2O, 3.33 μL 7.5% sodium bicarbonate solution (Life Technologies), and 16.67 μL 1× RPMI 1640 (Life Technologies) were premixed and stored at 4°C before experiments, as per manufacturer (Ibidi) instructions. Fifty microliters of 3.1 mg/mL Bovine collagen type I (Advanced BioMatrix) was added at time of seeding. A total of 16.67 μL of cells suspended in RPMI 1640 were mixed into the collagen/media mix to a final volume of 100 μL in 1.5 mg/mL bovine collagen I (6-fold dilution of RPMI 1640 cell suspension). Six microliters of this cell/matrix mix were used to load each viewing chamber. For cell lines in single culture or mixed culture, the final concentration of cells was 3×10^6 myeloma cells/mL. For patient primary cells, the densities were 7×10^6 cells/mL for multiple myeloma ($CD138^+$) and 1×10^6 cells/mL for mesenchymal cells. These cell densities were optimized to better reflect physiological cell density and maximize the number of cells in the observation chamber, while still maintaining enough separation to allow the individual identification of cells. Cell lines were seeded at lower density to account for their larger size and faster replication. The interval between mixing collagen with cells and media and seeding the chambers was kept below 5 minutes at ambient temperature to minimize collagen polymerization. After seeding, an additional 15 minutes at room temperature allowed adherent cells (HS-5 or patient stroma) to sink to the bottom of the 3D chamber and keep the same focal plane for subsequent live imaging. Slides were then incubated at 37°C, 5% CO_2 for 1 hour. Collagen polymerization was checked by visual inspection of fiber formation on an inverted phase contrast microscope with a ×20 objective lens. After gelation, reservoirs on each side of the slide were filled with 65 μL culture media. A total of 16.25 μL of 4× drug in culture media was dropped onto a filling port on the left reservoir and then an equal volume was immediately drawn out of the other filling port. Slides were then placed into incubator for live imaging. For each experiment, there was a control with no drug added, which was used to detect spontaneous cell death. For single culture experiments, chemotherapy was added 2 to 4 hours after cell seeding. For coculture experiments with adherent stroma (HS-5 or patient stroma), drugs were added 24 hours later to ensure stroma adhesion.

Continuous versus pulsed exposure. In experiments with continuous exposure, the drug was maintained in media for the duration of the experiment. If this duration exceeded 48 hours, the media on both reservoirs was completely removed, and replaced by fresh media, to which drug was added as previously described (16.25 μL at 4× concentration). In pulsed exposure experiments, the media on both reservoirs was completely removed and replaced by fresh media at the end of the pulsed exposure.

Imaging

Image acquisition. Two different models of fluorescence microscopes were used for the experiments here described: the first, JULI (Digital Bio), is a portable fluorescence microscope with bright field and red fluorescence capacities (ex/em 630 nm/660 nm), which was maintained inside a standard incubator for the duration of the experiments. The second platform was the EVOS FL (AMG), a bench top fluorescence microscope (red channel ex/em 531 nm/593 nm), which required the use of a stage-top heating stage/incubator (Ibidi), which maintained the cells at 37°C, 5% CO_2, and 80% humidity. For the experiments here described, images were acquired every 5-minute intervals. In experiments where the red fluorescent 8226/dsRed2 cell line was tested, or the cell-death molecular probe ethidium homodimer-1 (EthD-1) was used, both bright field

Published OnlineFirst December 5, 2013; DOI: 10.1158/0008-5472.CAN-13-2397

and red fluorescent channels were imaged, the first for changes in cell morphology and membrane motion, and the second for loss of innate fluorescence or activity of EthD-1, respectively.

Quantification of drug concentration over time within microfluidic device. To quantify the shape and stability of the drug gradient in the microfluidic device, we used a fluorophore-conjugated of the peptide HYD-1 (1.5 kDa) within the dose–response assay, a 3D gel matrix consisting of 1.5 mg/mL bovine collagen I with RPMI1640/MEM media was placed into the culture chamber of the Ibidi microfluidics device. After 45 minutes incubation at 37°C, reservoirs were filled with RPMI1640 media 10% heat inactivated FBS, 1% penicillin–streptomycin. FAM-HYD1 was diluted into media before replacing one fourth of the volume in the left reservoir with fluorescent drug solution (1/10 of stock). Fluorescence within the culture chamber was imaged in an EVOS FL microscope using the GFP filter (ex/em 470 nm/525 nm, ×5 objective) with heated stage and gas incubation (37°C, 5% CO_2). Images were acquired at 1-minute intervals for 24 hours.

Digital image analysis. With a stable drug gradient established across the main channel of the microfluidic slide, we arbitrarily divided the observation channel into 5 sections, or ROIs, each with an average drug concentration of 100%, 80%, 60%, 40%, and 20% of the concentration in the drug reservoir, respectively. Sectioning the channel into 5 areas was a compromise between a minimum number of cells in each area, and the rounding because of the averaging of the drug concentrations across each section. Dose–response was quantified with a macro developed for the software ImageJ (http://rsbweb.nih.gov/ij), further described. As discussed in the Results section, membrane-impermeable probes for detection of cell death, such as EthD-1, present a significant variation in the time for fluorescence acquisition after death in cell lines or patient samples. To avoid this confounding effect, we have developed a novel approach that identifies cell death based of motion of the membrane, described later.

Assessment of cell viability through membrane motion detection. We have observed that, although it was not possible to clearly discern a dead from a live cell based on the morphology in the bright field of a single image, all live cells suspended within the collagen matrix had observable membrane motion or shape changes, between 2 images taken in a 5-min interval. These morphological changes abruptly stopped before cell death, indicating that this feature could be exploited as a marker for cell death. We created a macro for the open source software ImageJ using the plugins TurboReg (20) and RunningZProjector (http://valelab.ucsf.edu/index.html). The macro quantifies the amount of cell membrane motion in the different regions of interest, and writes a file with this information for each frame, or time point. The source code of the macro is provided in the Supplementary Material. Briefly, the macro loads the stack of bright field images taken at 5-minute intervals, and aligns them using the plugin TurboReg. This action removes translational motion, such as sliding of the microfluidic chamber, as well as vibration. Next, the native ImageJ "background subtraction" function was used with parameters "rolling ball radius = 1 pixel" and "sliding parabolic" (21). Background subtraction served to normalize image sequences across different experiments and/or microscopes used to image the chambers, making cells appear as bright spots against a uniform dark background. Motion and small variations in cell membranes were detected using the plugin RunningZProjector. It detects the maximum pixel intensity across a 6-frame/slice interval, corresponding to 30 minutes. The original image was then subtracted from the maximum pixel intensity projection, resulting in an image where actively moving membranes appear as bright rings. ImageJ's Gaussian blur filter was used to convert these bright rings into spots that cover the entire cell, and produce the overlaid images shown in this article.

Validation of motion detection algorithm through fluorescence. Different fluorescent-labeling agents for cell viability were tested as live-imaging approaches for response to chemotherapy. However, cytotoxicity, photo bleaching, intercellular variability of delay between cell death and signal detection, and incomplete representation of viable/apoptotic/necrotic cell states added noise to the assay. A multiple myeloma cell line was stably transfected with dsRed2 (8226/dsRed2), and used as a reference to visually detect the cytotoxic effect of drugs through loss of red fluorescence. dsRed2 expression is an intrinsic marker for these cells: live cells will quickly loose fluorescence upon cell death because of membrane burst accompanied by release of cytoplasmic components, including the fluorescent protein.

Validation of motion detection algorithm through bioluminescence. NCI-H929 cells were seeded in 96-well plates in culture media or in a 3D collagen matrix with culture media added on top of the cell/collagen layer. In wells without collagen, 1.5×10^5 cells were resuspended in 50 μL of media for a final density of 3×10^6 cells/mL. To more closely resemble microfluidic assay conditions, 1.5×10^5 cells were suspended in 30 μL of 1.5 mg/mL collagen matrix and were left to polymerize at 37°C for 1 hour. Twenty microliters of media was then added as a separate phase on top of the cell/collagen layer. Melphalan was serially diluted in 2-fold steps to a final concentration range of 100 to 1.56 μmol/L in 7 rows. The same procedure was performed for bortezomib to final concentrations of 20 to 0.31 nmol/L. All conditions and controls were performed in triplicate. After 24 hours of continuous drug exposure at 37°C and 5% CO_2, 50 μL CellTiterGlo was added to each well and the plates were placed on an orbital shaker at room temperature for 10 minutes. Twenty minutes later, bioluminescence was measured at ambient temperature on a microplate reader. Percent cell viability was defined as luminescence normalized to controls at 24 hours.

Analysis of experimental data

The quantification of the dose–response of the cells in the experiment used Matlab's (MathWorks) function *lsqcurvefit*, which finds the coefficients that minimize the distance between a function and a set of data points. Details on the fitting procedure and equations used are presented in the Quick Guide to Equations and Assumptions.

Computational modeling of therapy

As a proof of principle, to exemplify the application of these *in vitro* chemosensitivity assays in estimating patient response

Published OnlineFirst December 5, 2013; DOI: 10.1158/0008-5472.CAN-13-2397

to therapy, we have used a computational model, previously described (22), to simulate a hypothetical single-agent bortezomib regimen in an animal model (s.c. NCI-H929 in SCID mouse), and for 4 patients whose multiple myeloma cells' sensitivity to bortezomib were tested *in vitro*. Implementation of the computational model of therapy is presented in the Quick Guide to Equations and Assumptions.

Results

Characterization of shape and duration of drug gradient

The first step of validating the *in vitro* platform was to determine the stability, and also the duration of any transients during the formation of the drug gradient across the observation chamber. For this purpose, we used a conjugate of the FAM and the 1.5 kDa peptide HYD-1, an experimental drug with direct toxicity to multiple myeloma cells (23). We used live imaging to quantify the fluorescence in images taken at 1-minute intervals during 18 hours (Fig. 1). The fluorescent signal gradient was stable for the interval of the experiment, and the transient time for its formation was shorter than the period between drug injection in the slide and start of imaging (~5–10′).

Loss of membrane motion is a reliable maker of cell death

A novel algorithm for detection of cell membrane motion was necessary to detect cell death in patient primary cells, because of the significant variation of the delay between cell death and membrane permeabilization, and acquisition of fluorescence from molecular probes. Supplementary Fig. S1 depicts the delay between the detection of cell death using the motion-detection algorithm, and loss of fluorescence in the stably transfected cell line 8226/dsRed2. Supplementary Fig. S2 exemplifies the delay of acquisition of the molecular probe EthD-1 red fluorescence in NCI-H929 cells.

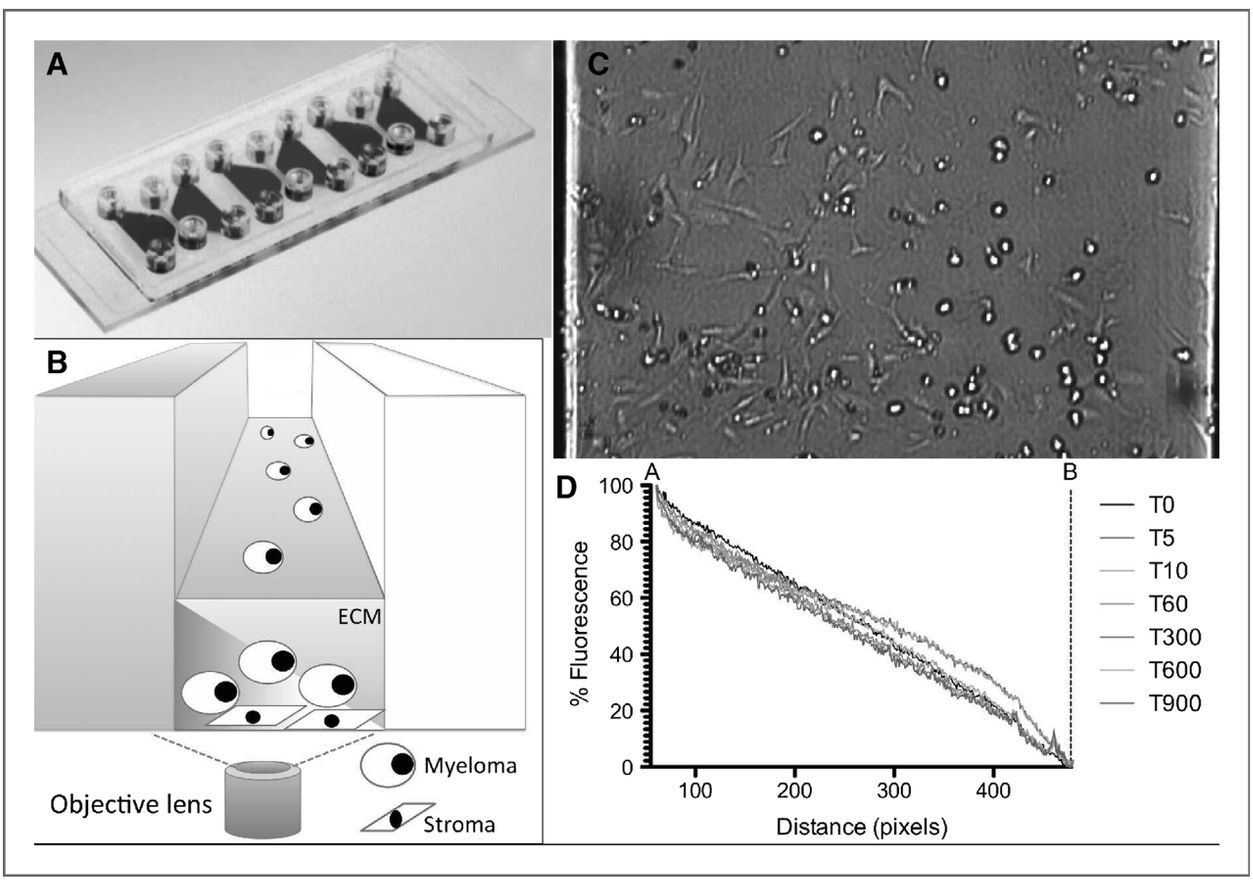

Figure 1. Schematic view of microfluidic assay used for *in vitro* reconstruction of bone marrow. A, each microfluidic chip contains 3 chambers, each of them composed of 2 side reservoirs, and one center observation chamber. Myeloma and stromal cells are loaded in the observation chamber simultaneously, resuspended in collagen. Overnight, the matrix gellifies and stromal cells adhere to the bottom of the chamber and stretch. B, one of the side reservoirs is filled with medium with a chemotherapeutic agent (left), whreas the other is filled with standard growth medium (right). The diffusion of the chemotherapeutic agent from one reservoir to the other creates a stable gradient across the observation chamber. C, the observation channel with the human multiple myeloma cell line NCI-H929 and adherent bone marrow–derived stromal cell line HS-5 is shown in bright field under a gradient of the necrosis-inducing peptide HYD-1. Note that multiple myeloma cells on the left (higher drug concentration) have died and became dark spots, whereas cells on the right (lower drug concentration) are still alive. D, a gradient of the fluorescent-conjugated peptide FAM-HYD1 was established and fluorescence quantified across the channel during 18 hours. Normalization and rescaling to the minimum and maximum concentration within the observation channel confirm the linear stable gradient during the 18-hour window of experiment.

Published OnlineFirst December 5, 2013; DOI: 10.1158/0008-5472.CAN-13-2397

Effect of the proteasome inhibitor bortezomib

The cell line NCI-H929 was exposed to a stable gradient of bortezomib (maximum concentration 10 nmol/L) for 24 hours, and a dose–response surface was created (Fig. 2A). According to these results, the bortezomib concentration that would lead to a 50% reduction in the number of live cells after 24 hours, compared with the initial time point, was ∼2.5 nmol/L. The concentration that would lead to a 50% reduction in the number of live cells, compared with the control at 24 hours was ∼1.9 nmol/L. The same cell line was seeded in a 96-well plate, in suspension or in collagen, and cell viability was measured using the ATP-based assay CellTiter-Glo (Fig. 2C). The Pearson test produced r values of 0.8905 and 0.8704 (P values 0.003 and 0.0049) for the correlation between the model and suspension, and collagen results, respectively.

Quantification of melphalan innate resistance in cell lines in single culture

The melphalan sensitive and resistant cell lines NCI-H929 and 8226/LR5 were exposed to stable gradients of melphalan for 24 hours (highest concentrations of 50 and 100 μmol/L, respectively) and chemosensitivity was quantified. The analysis of 8226/LR5 detected a subpopulation of sensitive cells (∼30%; Fig 3A), indicating that this cell line is actually heterogeneous, a possible explanation for the loss of resistance commonly observed when these cells are maintained in melphalan-free medium for many weeks (24). Melphalan concentration that induced 50% of death in cells (EC50) for 24 hours continuous exposure was ∼50 μmol/L for 8226/LR5 and ∼12 μmol/L for H929. Long-term exposure to lower, more physiological doses (10–20 μmol/L) of melphalan, however, indicated that, although all melphalan had been hydrolyzed in the first 24 hours in media, cell death continued to occur after 6 days of drug exposure (Supplementary Fig. S3).

Quantification environment-mediated melphalan resistance

Cell adhesion–mediated drug resistance is believed to be a major cause of minimal residual disease in multiple myeloma (18). This mechanism is caused by direct multiple myeloma–stroma cell adhesion, by paracrine loops of soluble factor secretion, or by multiple myeloma–extracellular matrix adhesion. To quantify the importance of multiple myeloma–stroma adhesion under physiological conditions (high density, in presence of ECM), the multiple myeloma cell line NCI-H929 was cocultured with the bone marrow–derived stromal cell

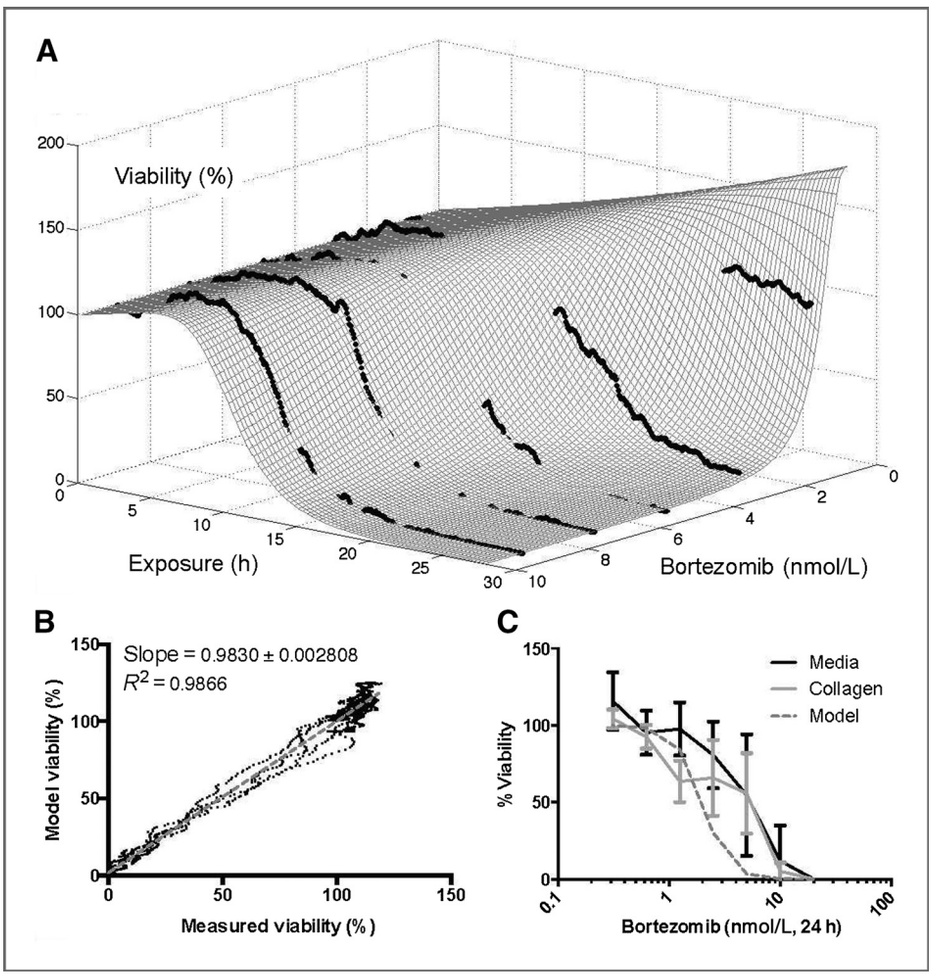

Figure 2. Quantification of sensitivity of the human myeloma cell line NCI-H929 to the proteasome inhibitor bortezomib. The microfluidic assay described in this project generates a series of measurements corresponding to cell viability at combination of exposure time and drug concentration. These data points in turn are fit to the mathematical expression of dose–response, equation A. A, sensitivity of the human myeloma cell line to the proteasome inhibitor bortezomib. B, goodness-of-fit of the mathematical model to the 1,670 data points. C, comparison of viability measurements at 24 hours between the mathematical model and a standard ATP-based bioluminescent assay, with NCI-H929 cells in suspension in media or in collagen, using a standard 96-well plate.

Published OnlineFirst December 5, 2013; DOI: 10.1158/0008-5472.CAN-13-2397

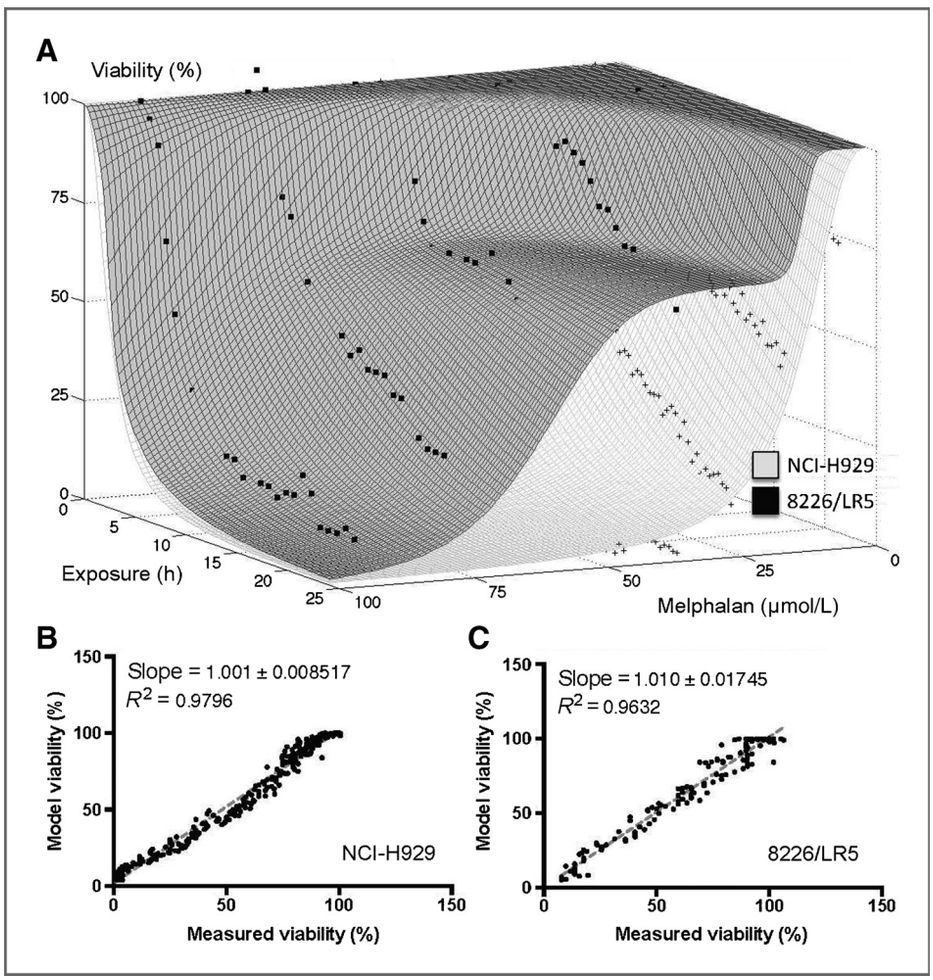

Figure 3. Intrinsic chemoresistance to melphalan. The human multiple myeloma cell lines 8226/LR5, selected by continuous exposure to melphalan, and NCI-H929 were exposed for a 24 hours continuous stable of gradient of melphalan in the microfluidic chamber. Although the cell line NCI-H929 was fit to a single population, the 8226/LR5 cell line was better fit by a 2-population curve, with approximately 70% of resistant cells and 30% of sensitive. This result indicates that the loss of chemoresistance of 8226/LR5 cells in absence of melphalan might be because of heterogeneity in this population.

line HS-5/GFP. A significant shift toward resistance was observed at later time points (~24 hours) and was most expressive around the concentration of 20 to 30 μmol/L (Fig. 4).

Continuous versus pulsed exposure to drugs

To exemplify the study of continuous versus pulsed exposure to drugs, 2 chambers with NCI-H929 cells were exposed to bortezomib for 24 hours. In one, the medium was replaced by drug-free medium, whereas in the other fresh medium with bortezomib was added. Being a reversible proteasome inhibitor, the results suggest that bortezomib-induced death stops upon drug withdrawal (Supplementary Fig. S4), unlike melphalan (Supplementary Fig. S3).

Melphalan chemosensitivity of primary multiple myeloma cells in single and coculture

From the 17 patient samples obtained so far in this protocol, the first 10 were used for development and optimization of the platform. The results of the 7 others are described here. We have exposed $CD138^+$-sorted primary multiple myeloma cells from patient 14, a newly diagnosed patient, for 48 hours to a stable gradient of 25 μmol/L melphalan in single and coculture, with patient-derived stroma. As shown in Fig. 5, adhesion to stroma significantly increased the survival of multiple myeloma cells, shifting the 48 hours EC_{50} from 2 μmol/L in single culture to 12 μmol/L in coculture. This effect could be circumvented by combination of a proteasome inhibitor at sublethal levels (Fig. 6 and Supplementary Video S1; ref. 25).

Melphalan and bortezomib chemosensitivity among patients with multiple myeloma

Supplementary Fig. S5 depicts the *in vitro* chemosensitivity of 3 patients with multiple myeloma to melphalan in single culture: patient 14, patient 11 (smoldering myeloma), and patient 12 (relapsed after bone marrow transplantation). The EC_{50}s at 24-hour exposure were 4 μmol/L for patients 14 and 12 and 1 μmol/L for patient 11. However, the percentage surviving cells at 20 μmol/L, a more physiological concentration of high-dose melphalan treatment, was 30% for patient 12, 11% for patient 14, and 4% for patient 11. Fig. 7 represents bortezomib chemosensitivity of patients 11, 12, 13 (newly diagnosed), and 17 (smoldering myeloma). For patients 11 and 12, EC_{50} after 24 hours continuous exposure was below 2 nmol/L; however, at higher concentrations, multiple myeloma cells from patient 11 were significantly more resistant: 30% live cells at 50 nmol/L bortezomib for patient 11 and ~8% for patient 12. Twenty-

Published OnlineFirst December 5, 2013; DOI: 10.1158/0008-5472.CAN-13-2397

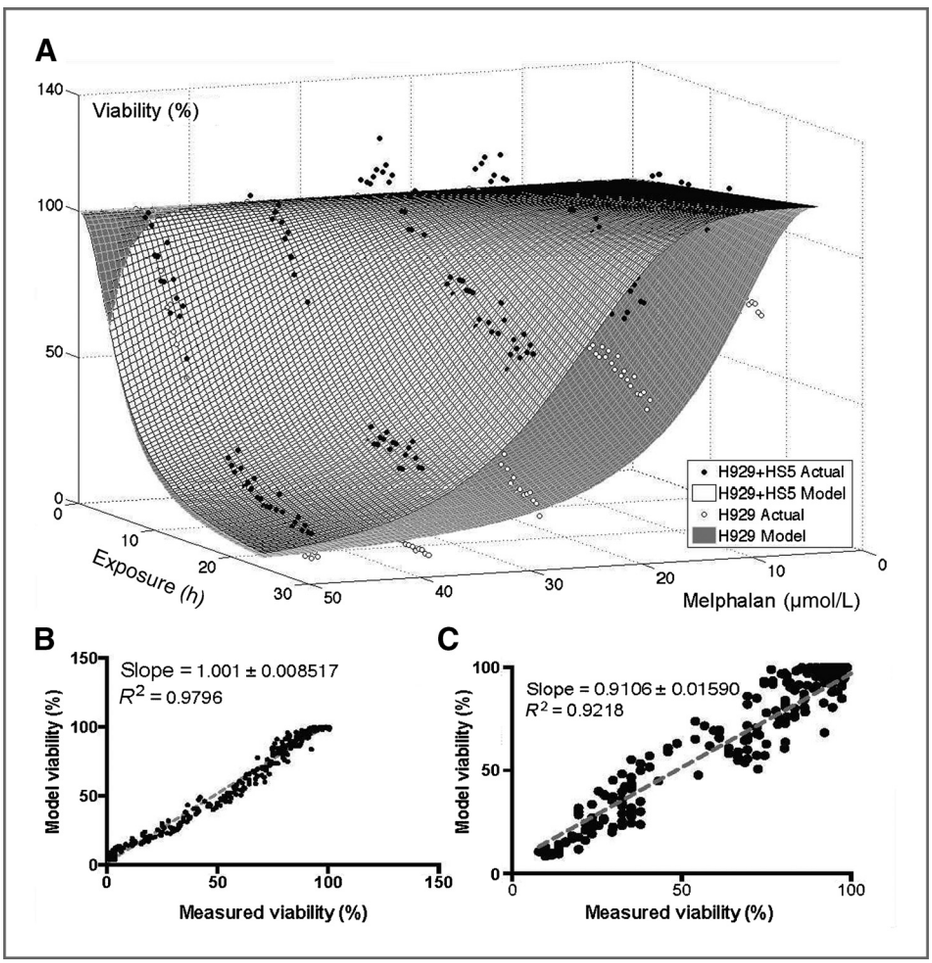

Figure 4. Effect of cell adhesion mediated drug resistance in the multiple myeloma cell line NCI-H929 treated with melphalan. A, the coculture of the NCI-H929 human multiple myeloma cell line with the human bone marrow–derived stromal cell line HS-5 confers increased resistance to melphalan. Melphalan concentration and exposure required to reduce viability in 50% (kR and kT, respectively) increase from 28 to 40 μmol/L and 12 to 15 hours, respectively. B and C, linear regression of fit and actual experimental points for both experiments.

four-hour EC_{50} for patient 13 was ~10 nmol/L, whereas EC_{50} was not reached with the sample from patient 17.

Extrapolation of *in vitro* data into *in vivo* and clinical response

By parameterizing equation C with values obtained from fitting equation A to the *in vitro* dose–response data, it is possible to simulate how a tumor mass would respond to a therapeutic regimen. As an example, the subcutaneous mouse model severe combined immunodeficient (SCID), when implanted with the cell line NCI-H929, develops a tumor that grows 45-fold in 20 days (26). When treated with 1 mg/kg bortezomib twice a week, the tumor growth is reduced, and tumors are 20-fold bigger at day 20 than at implantation (27). From the bortezomib *in vitro* chemosensitivity assay with the cell line NCI-H929 (Fig. 2), the parameters from equation C were: $IC_{50Rx} = 10.35$ nmol/L, $IC_{50\Delta T} = 10.38$ hours, exp $Rx = 2.7$, and exp $T = 7.1$. Supplementary Fig. 6 depicts the computational simulation of the tumor growth under control conditions, under a bi-weekly treatment with 1 mg/kg of bortezomib (which leads to a stable blood concentration of 0.4 nmol/L; ref. 28), and a hypothetical regimen where mice received a pulsed therapy with the same AUC, with bi-weekly injections of bortezomib every other week (therapy holidays). The simulated tumor would have increased 53.4-fold in control conditions (Pearson $r = 0.9762$), 18-fold in standard bortezomib treatment (Pearson $r = 0.9869$), and 5-fold in the hypothetical pulsed regimen. The same approach was used to simulate the response of patients 11, 12, 13, and 17 to a single-agent regimen of bortezomib (1.3 mg/m^2; Supplementary Fig. 7). In this regimen, plasma concentration stabilizes at ~1 nmol/L (4), and according to simulations, would achieve complete response in patients 11 an 12, relapse in patient 17, and no response in patient 13.

Discussion

In this work, we have described an interdisciplinary platform to study preclinical drug activity in primary multiple myeloma cells. First, multiple myeloma cells are embedded in a microfluidic chamber that recapitulates the bone marrow microenvironment, including high-cell density, extracellular matrix, and patient-derived stromal cells. A linear and stable drug gradient is established across the chamber, which is then imaged sequentially in bright field. A digital image analysis algorithm detects live multiple myeloma cells by the motion of cell membrane: upon death this activity ceases. The

Published OnlineFirst December 5, 2013; DOI: 10.1158/0008-5472.CAN-13-2397

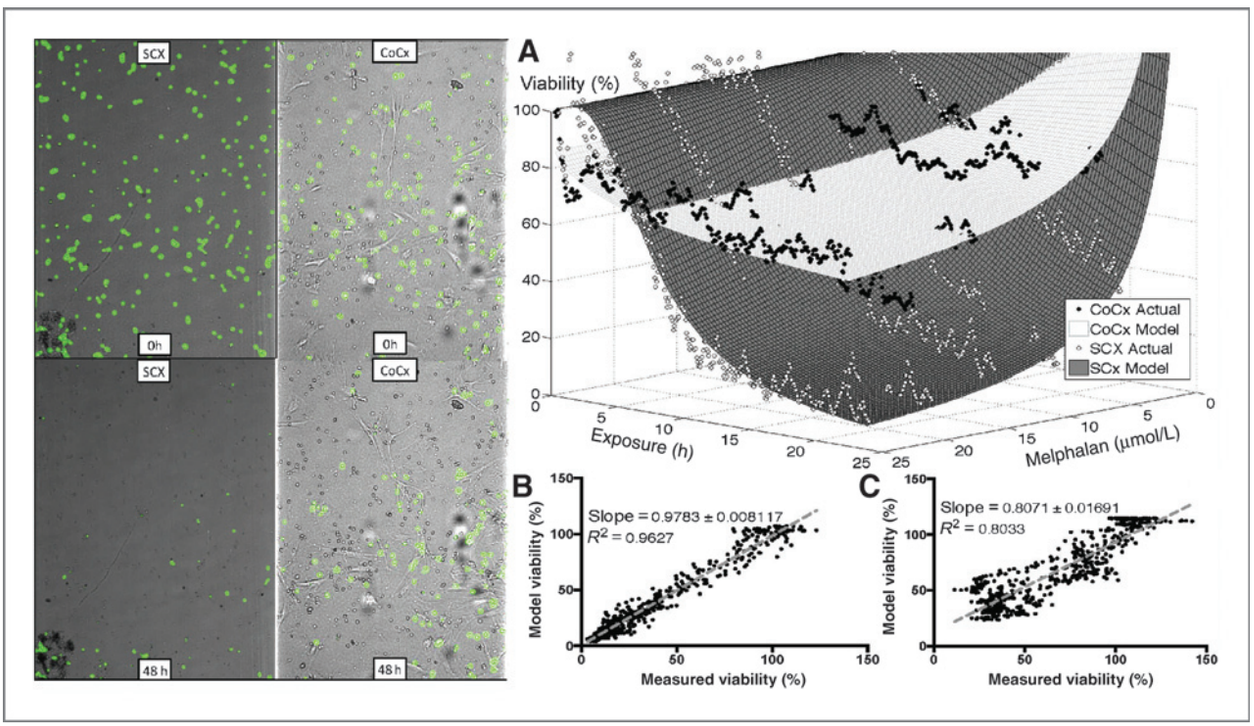

Figure 5. Primary multiple myeloma cells in coculture with patient stroma are significantly more resistant to melphalan. Patient 14 is a newly diagnosed patient. Multiple myeloma cells were sorted ($CD138^+$) from bone marrow aspirate and seeded into microfluidic chamber in single (SCX, 0 hour) or coculture with patient stromal cells (CoCx, 0 hour). Digital image analysis identifies live cells and pseudo-colors as green. A stable linear gradient of melphalan was established across observation channel: 25 μmol/L on the left, 0 μmol/L on the right, and cells were imaged every 5 minutes for 48 hours. After 48 hours, almost all multiple myeloma cells are dead in single culture (SCX, 48 hours), whereas a significant number of multiple myeloma cells are still alive in coculture with stroma (CoCx, 48 hours). A, dose–response surfaces built using measurements of viability in single (SCX) and coculture (CoCx). B and C, goodness-of-fit of dose–response surfaces (model) and actual data points for single culture (B) and coculture (C).

measurements of viability, at different concentrations and time points, are fit to mathematical models of chemosensitivity. These models can represent one or multiple subpopulations, and can be empirical or mechanistic. The data from these experiments can thus be used to parameterize mathematical models to simulate clinical outcome.

This platform overcomes some major limitations of preclinical assays using primary cancer cells. It has long been known

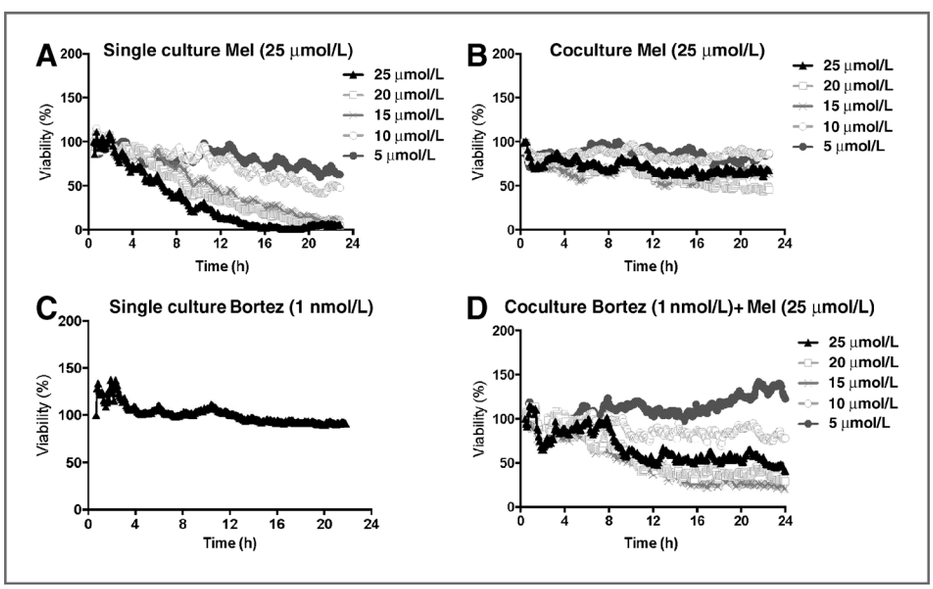

Figure 6. Quantification of bortezomib-induced EMDR circumvention in primary multiple myeloma cells. Patient 14 is a newly diagnosed patient. Multiple myeloma cells were sorted ($CD138^+$) from bone marrow aspirate and seeded into microfluidic chamber in single and coculture with adherent stromal cells ($CD138^-$). A and B, in single culture (A), multiple myeloma cells are significantly more sensitive than in coculture (B). A dose–response assay with bortezomib indicated that 1 nmol/L was the highest concentration that did not cause multiple myeloma cell death (C) during the 24-hour period. By combining a stable gradient of melphalan with a uniform concentration of bortezomib, the chemosensitive phenotype is restored in coculture (D).

Published OnlineFirst December 5, 2013; DOI: 10.1158/0008-5472.CAN-13-2397

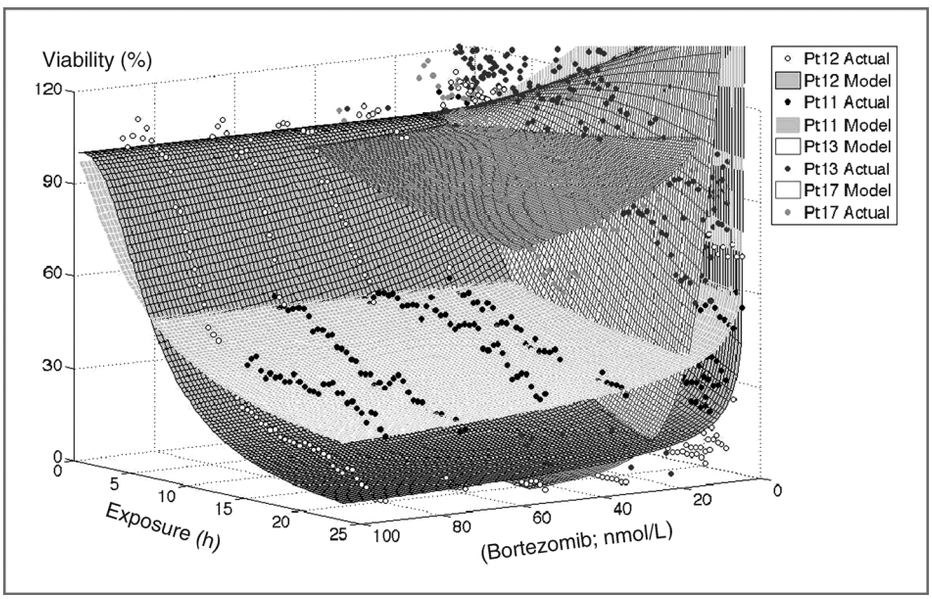

Figure 7. *In vitro* response of primary multiple myeloma cells to bortezomib in single culture 3D collagen matrix. Patient 11 was a smoldering/standard-risk patient, and thus never previously treated with bortezomib. Patient 12 was a relapsed/standard-risk patient previously treated with bortezomib-based regimens and high-dose melphalan followed by bone marrow transplantation. Patient 12′s bortezomib-based induction regimen (bortezomib/lenalidomide/dexamethasone) occurred 3 years before the biopsy used for this *in vitro* assay. Patient 13 was a newly diagnosed/high-risk patient, whereas patient 17 was a smoldering myeloma patient.

that extracellular matrix and stroma are major components of chemoresistance in many tumors. However, the inclusion of these elements significantly increases the complexity of dose–response assays, often requiring the separation between cancer and stromal cells, by matrix digestion and/or flow sorting (29). Also, viability assays are often destructive or cytotoxic, if carried for long periods of time, limiting the information acquired in the temporal dimension. In the here described assay, multiple myeloma cells, stroma, and matrix are never separated, and no cytotoxic agents are used to determine cell viability, thus allowing longitudinal studies of drug activity without interfering with the microenvironment.

In cancers such as multiple myeloma, where a few million cells are obtainable per patient biopsy, it is important to minimize the number of cells per experimental condition, which is in the order of 1,000 to 10,000 cells in this assay. The poor clonal efficiency of multiple myeloma cells, as well as their spontaneous death *in vitro* (6), suggest that experiments with these samples be performed in the first few days after the biopsy. By studying the effect of long-term exposure and drug withdrawal in human multiple myeloma cell lines, we have created mechanistic theoretical models of the drug activity (2). Once a model is generated for a particular drug, the data from patient samples are used to parameterize and extrapolate the response for longer periods of time.

As shown for bortezomib-induced melphalan sensitization in coculture (Fig. 6), this system can be used to study drug interactions (30). The addition of the time dimension, instead of fixed time points, would allow the study of time-shifted drug combinations, such as, for instance, nuclear export agents and doxorubicin (31). Combination indices (30) may be obtained by adding the 2 drugs being studied on the same reservoir, which will induce 2 superimposed drug gradients.

This assay allows the observation of individual cells. Thus, it is possible to assess the heterogeneity of drug–response by plotting in a histogram the AUC at the moment of death of each individual cell. Further improvements in the digital image analysis algorithm could identify and track individual cells from their original replication until their death. By combining this information with the dose–response surfaces, it would be possible to determine if particular drugs and concentrations are capable of maintaining a tumor burden quiescent, or in a balance between proliferation and death (32, 33).

These preliminary results describe a framework to better understand the dynamics of interactions between tumor and stroma in response to therapeutic agents *in vitro*. These assays can be performed in a middle- to high-throughput manner, and significantly reduce the complexity of working with patient primary cells in reconstructions of the tumor microenvironment. Ultimately, this may become a platform for personalized preclinical estimation of drug efficacy in cancer.

Future directions are to standardize methods to extrapolate *in vitro* predictions into clinical outcome. We will also explore the application of alternative therapeutic regimens of drug combinations, proposed by data extrapolated from this *in vitro* system, and simulated using evolutionary computational models (34, 35). We hypothesize that, patient-specific computational models, parameterized by in *vitro* platforms as the here described, could be combined with genomic (36) datasets to better understand the dynamics that underlie evolution of drug resistance in patients with multiple myeloma. Understanding these dynamics would not only allow accurate predictions of response, but also suggest the best therapeutic strategies for each patient, and continue adjusting these strategies as needed.

Disclosure of Potential Conflicts of Interest

No potential conflicts of interest were disclosed.

Authors' Contributions

Conception and design: Z.P. Khin, M.L.C. Ribeiro, K. Shain, A.S. Silva
Development of methodology: Z.P. Khin, M.L.C. Ribeiro, T. Jacobson, K. Shain, A.S. Silva
Acquisition of data (provided animals, acquired and managed patients, provided facilities, etc.): Z.P. Khin, M.L.C. Ribeiro, T. Jacobson, A.S. Silva

Analysis and interpretation of data (e.g., statistical analysis, biostatistics, computational analysis): Z.P. Khin, T. Jacobson, K. Shain, A.S. Silva
Writing, review, and/or revision of the manuscript: Z.P. Khin, T. Jacobson, L. Hazlehurst, L. Perez, R. Baz, K. Shain, A.S. Silva
Administrative, technical, or material support (i.e., reporting or organizing data, constructing databases): K. Shain
Study supervision: A.S. Silva

Acknowledgments

The authors thank the patients at H. Lee Moffitt Cancer Center who provided clinical samples for our *in vitro* assays as well as consented access to the their clinical data through the Total Cancer Care database.

Grant Support

This research was funded by the State of Florida's Bankhead-Coley Team Science Grant (2BT03), the National Institutes of Health/National Cancer Institute (1R21CA164322-01), and the H. Lee Moffitt Cancer Center Physical Sciences in Oncology (PSOC) Transnetwork Grant (U54CA143803).

The costs of publication of this article were defrayed in part by the payment of page charges. This article must therefore be hereby marked *advertisement* in accordance with 18 U.S.C. Section 1734 solely to indicate this fact.

Received August 21, 2013; accepted October 20, 2013; published OnlineFirst December 5, 2013.

References

1. Samuels BL, Bitran JD. High-dose intravenous melphalan: a review. J Clin Oncol 1995;13:1786–99.
2. Gardner SN. A mechanistic, predictive model of dose-response curves for cell cycle phase-specific and -nonspecific drugs. Cancer Res 2000;60:1417–25.
3. Ogawa Y, Tobinai K, Ogura M, Ando K, Tsuchiya T, Kobayashi Y, et al. Phase I and II pharmacokinetic and pharmacodynamic study of the proteasome inhibitor bortezomib in Japanese patients with relapsed or refractory multiple myeloma. Cancer Sci 2008;99:140–4.
4. Reece DE, Sullivan D, Lonial S, Mohrbacher AF, Chatta G, Shustik C, et al. Pharmacokinetic and pharmacodynamic study of two doses of bortezomib in patients with relapsed multiple myeloma. Cancer Chemother Pharmacol 2011;67:57–67.
5. Ishii T, Seike T, Nakashima T, Juliger S, Maharaj L, Soga S, et al. Antitumor activity against multiple myeloma by combination of KW-2478, an Hsp90 inhibitor, with bortezomib. Blood Cancer J 2012;2:e68.
6. Suggitt M, Bibby MC. 50 years of preclinical anticancer drug screening: empirical to target-driven approaches. Clinical Cancer Research 2005;11:971–81.
7. Von Hoff DD, Clark GM, Stogdill BJ, Sarosdy MF, O'Brien MT, Casper JT, et al. Prospective clinical trial of a human tumor cloning system. Cancer Res 1983;43:1926–31.
8. Pellat-Deceunynk C, Amiot M, Bataille R, Van Riet I, Van Camp B, Omede P, et al. Human myeloma cell lines as a tool for studying the biology of multiple myeloma: a reappraisal 18 years after. Blood 1995;86:4001–2.
9. Hokanson JA, Brown BW, Thompson JR, Drewinko B, Alexanian R. Tumor growth patterns in multiple myeloma. Cancer 1977;39:1077–84.
10. Chmielecki J, Foo J, Oxnard GR, Hutchinson K, Ohashi K, Somwar R, et al. Optimization of dosing for EGFR-mutant non-small cell lung cancer with evolutionary cancer modeling. Sci Transl Med 2011;3:90ra59.
11. Tang M, Gonen M, Quintas-Cardama A, Cortes J, Kantarjian H, Field C, et al. Dynamics of chronic myeloid leukemia response to long-term targeted therapy reveal treatment effects on leukemic stem cells. Blood 2011;118:1622–31.
12. Gardner SN, Fernandes M. New tools for cancer chemotherapy: computational assistance for tailoring treatments. Mol Cancer Ther 2003;2:1079–84.
13. Salmon SE, Hamburger AW, Soehnlen B, Durie BG, Alberts DS, Moon TE. Quantitation of differential sensitivity of human-tumor stem cells to anticancer drugs. N Engl J Med 1978;298:1321–7.
14. Suggitt M, Bibby MC. 50 years of preclinical anticancer drug screening: empirical to target-driven approaches. Clin Cancer Res 2005;11:971–81.
15. Kirshner J, Thulien KJ, Martin LD, Debes Marun C, Reiman T, Belch AR, et al. A unique three-dimensional model for evaluating the impact of therapy on multiple myeloma. Blood 2008;112:2935–45.
16. Durie BG, Jacobson J, Barlogie B, Crowley J. Magnitude of response with myeloma frontline therapy does not predict outcome: importance of time to progression in southwest oncology group chemotherapy trials. J Clin Oncol 2004;22:1857–63.
17. Harousseau JL, Attal M, Avet-Loiseau H. The role of complete response in multiple myeloma. Blood 2009;114:3139–46.
18. Meads MB, Gatenby RA, Dalton WS. Environment-mediated drug resistance: a major contributor to minimal residual disease. Nat Rev Cancer 2009;9:665–74.
19. Meads MB, Hazlehurst LA, Dalton WS. The bone marrow microenvironment as a tumor sanctuary and contributor to drug resistance. Clin Cancer Res 2008;14:2519–26.
20. Thevenaz P, Ruttimann UE, Unser M. A pyramid approach to subpixel registration based on intensity. IEEE Trans Image Process 1998;7:27–41.
21. Sternberg SR. Biomedical image processing. Computer 1983;16:22–34.
22. Silva AS, Kam Y, Khin ZP, Minton SE, Gillies RJ, Gatenby RA. Evolutionary approaches to prolong progression-free survival in breast cancer. Cancer Res 2012;72:6362–70.
23. Nair RR, Emmons MF, Cress AE, Argilagos RF, Lam K, Kerr WT, et al. HYD1-induced increase in reactive oxygen species leads to autophagy and necrotic cell death in multiple myeloma cells. Mol Cancer Ther 2009;8:2441–51.
24. Bellamy WT, Dalton WS, Gleason MC, Grogan TM, Trent JM. Development and characterization of a melphalan-resistant human multiple myeloma cell line. Cancer Res 1991;51:995–1002.
25. Yanamandra N, Colaco NM, Parquet NA, Buzzeo RW, Boulware D, Wright G, et al. Tipifarnib and bortezomib are synergistic and overcome cell adhesion-mediated drug resistance in multiple myeloma and acute myeloid leukemia. Clin Cancer Res 2006;12:591–9.
26. Nakashima T, Ishii T, Tagaya H, Seike T, Nakagawa H, Kanda Y, et al. New molecular and biological mechanism of antitumor activities of KW-2478, a novel nonansamycin heat shock protein 90 inhibitor, in multiple myeloma cells. Clin Cancer Res 2010;16:2792–802.
27. Ishii T, Seike T, Nakashima T, Juliger S, Maharaj L, Soga S, et al. Antitumor activity against multiple myeloma by combination of KW-2478, an Hsp90 inhibitor, with bortezomib. Blood Cancer J 2012;2:e68.
28. Williamson MJ, Silva MD, Terkelsen J, Robertson R, Yu L, Xia C, et al. The relationship among tumor architecture, pharmacokinetics, pharmacodynamics, and efficacy of bortezomib in mouse xenograft models. Mol Cancer Ther 2009;8:3234–43.
29. Misund K, Baranowska KA, Holien T, Rampa C, Klein DC, Borset M, et al. A method for measurement of drug sensitivity of myeloma cells co-cultured with bone marrow stromal cells. J Biomol Screen 2013;18:637–46.
30. Chou TC. Theoretical basis, experimental design, and computerized simulation of synergism and antagonism in drug combination studies. Pharmacol Rev 2006;58:621–81.
31. Turner JG, Marchion DC, Dawson JL, Emmons MF, Hazlehurst LA, Washausen P, et al. Human multiple myeloma cells are sensitized to topoisomerase II inhibitors by CRM1 inhibition. Cancer Res 2009;69:6899–905.
32. Wells A, Griffith L, Wells JZ, Taylor DP. The dormancy dilemma: quiescence versus balanced proliferation. Cancer Res 2013;73:3811–6.
33. San-Miguel JF, Mateos MV. Can multiple myeloma become a curable disease? Haematol-Hematol J 2011;96:1246–8.
34. Silva AS, Gatenby RA. A theoretical quantitative model for evolution of cancer chemotherapy resistance. Biol Direct 2010;5:25.
35. Silva AS, Kam Y, Khin ZP, Minton SE, Gillies RJ, Gatenby RA. Evolutionary approaches to prolong progression-free survival in breast cancer. Cancer Res 2012;72:6362–70.
36. Landau DA, Carter SL, Stojanov P, McKenna A, Stevenson K, Lawrence MS, et al. Evolution and impact of subclonal mutations in chronic lymphocytic leukemia. Cell 2013;152:714–26.

Published OnlineFirst December 5, 2013; DOI: 10.1158/0008-5472.CAN-13-2397

Cancer Research
The Journal of Cancer Research (1916–1930) | The American Journal of Cancer (1931–1940)

AACR American Association for Cancer Research

A Preclinical Assay for Chemosensitivity in Multiple Myeloma

Zayar P. Khin, Maria L.C. Ribeiro, Timothy Jacobson, et al.

Cancer Res 2014;74:56-67. Published OnlineFirst December 5, 2013.